Environmental Science & Technology

pubs.acs.org/est

Article

Degradation of Perfluoroalkyl Ether Carboxylic Acids with Hydrated Electrons: Structure−Reactivity Relationships and Environmental Implications

Michael J. Bentel, Yaochun Yu, Lihua Xu, Hyuna Kwon, Zhong Li, Bryan M. Wong, Yujie Men, and Jinyong Liu*

Cite This: *Environ. Sci. Technol.* 2020, 54, 2489−2499

Read Online

ACCESS | Metrics & More | Article Recommendations | Supporting Information

ABSTRACT: This study explores structure−reactivity relationships for the degradation of emerging perfluoroalkyl ether carboxylic acid (PFECA) pollutants with ultraviolet-generated hydrated electrons (e_{aq}^-). The rate and extent of PFECA degradation depend on both the branching extent and the chain length of oxygen-segregated fluoroalkyl moieties. Kinetic measurements, theoretical calculations, and transformation product analyses provide a comprehensive understanding of the PFECA degradation mechanisms and pathways. In comparison to traditional full-carbon-chain perfluorocarboxylic acids, the distinct degradation behavior of PFECAs is attributed to their ether structures. The ether oxygen atoms increase the bond dissociation energy of the C−F bonds on the adjacent $-CF_2-$ moieties. This impact reduces the formation of H/F-exchanged polyfluorinated products that are recalcitrant to reductive defluorination. Instead, the cleavage of ether C−O bonds generates unstable perfluoroalcohols and thus promotes deep defluorination of short fluoroalkyl moieties. In comparison to linear PFECAs, branched PFECAs have a higher tendency of H/F exchange on the tertiary carbon and thus lower percentages of defluorination. These findings provide mechanistic insights for an improved design and efficient degradation of fluorochemicals.

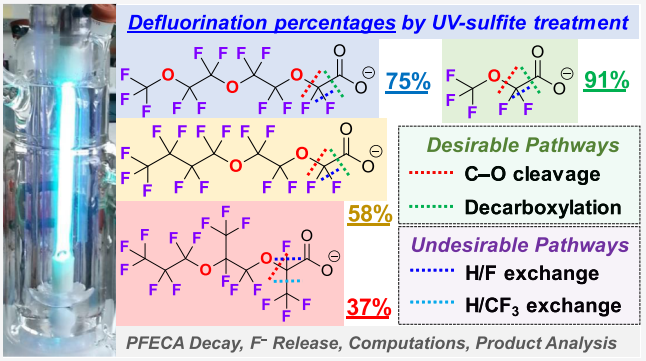

INTRODUCTION

Since the 1940s, per- and polyfluoroalkyl substances (PFASs) have been extensively used in a wide range of applications because of their unique properties (e.g., hydrophobicity, lipophobicity, and thermal stability) as well as their relative ease in chemical design and synthesis.[1−5] The highly stable C−F bond makes PFAS molecules recalcitrant to natural and engineered degradation,[6] leading to global PFAS pollution[7] and worldwide efforts on PFAS regulation.[8−11] Fluorochemical industries have been phasing out the production and use of some legacy PFASs [e.g., perfluorooctanoic acid (PFOA)][2,12] because of their heavy pollution of the environment and high toxicities to humans.[13,14] Perfluoroalkyl ether carboxylic acids (PFECAs) that contain ether C−O bonds in molecules have been developed as "less bioaccumulative alternatives" to full-carbon-chain predecessor PFASs.[15] However, toxicological studies have revealed an even higher bioaccumulation potential and toxicity of some PFECAs than PFOA,[16−19] and PFECAs have been recognized as a new class of contaminants of emerging concern (Figure 1).[20−23] At some sites in North America and in Europe, PFECAs have been detected in much higher concentrations than legacy PFASs.[24,25] Furthermore, because of the facile synthesis of PFECAs from flexible choices of fluoroalkene oxide building blocks (e.g., Figure S1)[26] and the formation of byproducts,[27] the diversity of PFECA contaminants identified in the environment has been rapidly increasing.[27−29]

While physical separation methods (e.g., carbon adsorption, ion exchange, and membrane filtration) enable rapid PFAS removal from contaminated water,[30] concentrated PFASs in carbon/resin regeneration waste and membrane rejects still require degradation treatment. Various novel methods, such as electrochemical,[31] sonochemical,[32] radiolytic,[33] plasmatic,[34] and other oxidative and reductive approaches,[30,35] have been primarily developed for the degradation of PFOA and perfluorooctane sulfonic acid. A few studies have investigated the destruction of selected PFECAs, including sonochemical oxidation with persulfate,[36] photocatalytic oxidation with

Received: September 29, 2019
Revised: December 27, 2019
Accepted: January 12, 2020
Published: January 30, 2020

https://dx.doi.org/10.1021/acs.est.9b05869
Environ. Sci. Technol. 2020, 54, 2489−2499

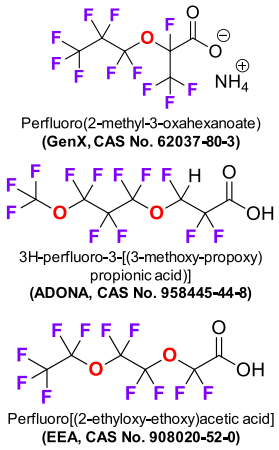

Figure 1. Examples of commercial perfluorinated (GenX and EEA) and polyfluorinated (ADONA) ether carboxylic acids detected in the environment.

phosphotungstic acid under pressurized O_2,[37] and reduction with ultraviolet (UV)-generated hydrated electrons (e_{aq}^-).[38,39] These early studies have revealed a variety of mechanistic insights on PFECA degradation. In particular, reductive degradation of branched PFECAs (e.g., GenX in Figure 1) using e_{aq}^- is much more effective than oxidative degradation using sulfate radicals.[38,39] However, a systematic understanding of reaction pathways and structure−reactivity relationships has not yet been established.

Recently, our research team has systematically studied the reductive defluorination of full-carbon-chain PFASs by e_{aq}^- produced from aqueous sulfite under UV irradiation.[40] The degradation mechanisms for perfluorocarboxylic acids (PFCAs) and fluorotelomer carboxylic acids (FTCAs) are significantly different. FTCAs ($R_F-CH_2CH_2-COO^-$, where R_F represents the fluorocarbon moiety) are much more recalcitrant than PFCAs (R_F-COO^-), especially when the chain length of R_F is short. The incomplete defluorination of PFCAs can also be attributed to the formation of polyfluorinated $R_F-CH_2-COO^-$ products.[40] These findings indicate the importance of a direct linkage between R_F and $-COO^-$ to allow an effective degradation of full-carbon-chain PFASs using e_{aq}^-. In comparison, the flexible incorporation of ether linkages in PFECAs generates various oxygen-segregated fluoroalkyl moieties, which can be either branched or linear in variable lengths. This novel structural diversity raises fundamental questions regarding mechanistic understanding and pollution control: (1) Mechanistically, what roles do the ether C−O bond and other structural features play in PFECA degradation using e_{aq}^-? (2) Practically, in comparison to full-carbon-chain PFCAs, can PFECAs be treated with a higher effectivity by these promising reductive technologies?

To answer these questions, we investigated the reductive defluorination of 10 PFECAs with (i) varying numbers of ether C−O bonds, (ii) varying chain lengths of oxygen-segregated fluoroalkyl moieties, and (iii) branched versus linear fluoroalkyl structures. To achieve a comprehensive understanding, we conducted kinetic measurements on parent compound decay and fluoride ion (F^-) release, theoretical calculations on C−F/C−O bond dissociation energies, spontaneous bond cleavage upon reaction with e_{aq}^-, and transformation product (TP) analyses with high-resolution mass spectrometry. These results collectively reveal and confirm novel mechanistic insights into PFECA degradation. These findings will advance treatment technologies for existing PFECA pollutants and facilitate the molecular design of fluorochemicals with enhanced degradability.

MATERIALS AND METHODS

This study utilized 10 PFECAs with fine-tuned structural variability in 4 categories (**A1** through **D2** in Table 1) and 2

Table 1. Overall Defluorination Percentages of PFECAs after 48 Hours of Reaction[a]

Entry	Structure	*n*	deF%
	A. *Branched (HFPO oligomers)*		
A1	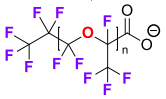	1	44.9 ± 5.3
A2		2	36.5 ± 2.9
A3		3	30.8 ± 4.2
	B. *Mono-ether with head CF_3O-*		
B1	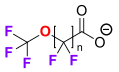	1	90.5 ± 2.1
B2		2	61.2 ± 7.5
B3		3	52.3 ± 3.1
	C. *TFEO oligomers with head CF_3O-*		
C1	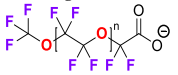	1	82.3 ± 4.4
C2		2	75.0 ± 3.8
	D. *TFEO oligomers with head C_4F_9O-*		
D1	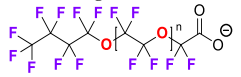	1	58.0 ± 4.0
D2		2	65.4 ± 6.3
	E. *Full-carbon-chain PFCAs*[b]		
E1		1	98.2 ± 5.0
E2		2-10	54.5 ± 3.5

[a]Reaction conditions: PFAS (0.025 mM), Na_2SO_3 (10 mM), carbonate buffer (5 mM), 254 nm irradiation (a 18 W low-pressure Hg lamp for 600 mL solution) at pH 9.5 and 20 °C. [b]Data from ref 40 for comparison. The average and standard deviation of the deF % value for n = 2−10 is based on 27 data points (nine PFCA structures with triplicates).

special compounds [trifluoropyruvate (TFPy) $CF_3-CO-COO^-$ and trifluoromethoxyacetate (TFMOA) $CF_3-O-CH_2-COO^-$] for mechanistic investigations. Detailed information on these chemicals is included in the Supporting Information. Preparation of PFECA stock solutions, photochemical reaction settings, sample analysis, and theoretical calculations have been fully described in our previous work (Open Access).[40] We used consistent reaction conditions to compare the degradation behavior between PFECAs and traditional full-carbon-chain PFCAs. Briefly, the photochemical degradation of individual PFECAs was carried out in 600 mL closed-system batch reactors equipped with a low-pressure mercury lamp (254 nm, 18 W, enclosed in a quartz immersion well). Both the reactor and immersion well were connected to circulating cooling water at 20 °C. The reaction mixture contained 25 μM PFECA, 10 mM Na_2SO_3, and 5 mM $NaHCO_3$, and the pH was adjusted to 9.5 with NaOH. The released F^- was measured with an ion-selective electrode, which has been validated for quantification accuracy by ion chromatography (IC). All reactions were conducted in

https://dx.doi.org/10.1021/acs.est.9b05869
Environ. Sci. Technol. 2020, 54, 2489−2499

triplicates of operations from the preparation of stock solution to the quantification of the defluorination percentage (deF %), which is defined as

$$\text{deF } \% = \frac{C_{F^-}}{C_0 \times N_{C-F}} \times 100\% \quad (1)$$

where C_{F^-} is the molar concentration of F^- released in solution, C_0 is the initial molar concentration of parent PFECAs, and N_{C-F} is the number of C−F bonds in the parent PFECA molecule. Reaction samples were analyzed with a liquid chromatography−triple quadrupole mass spectrometer (LC−MS/MS) for the quantification of parent compounds and TPs that have pure chemicals available as analytical standards. A liquid chromatography−high-resolution mass spectrometer (LC-HRMS) was also used for the screening of TPs without analytical standards. The quality assurance and quality control of our MS analyses have been addressed previously,[40] with new details provided in the Supporting Information for the PFECA degradation samples. Small ionic species including trifluoroacetate, TFPy, oxalate, perfluoromethoxyacetate (PFMOA, $CF_3-O-CF_2-COO^-$), and TFMOA ($CF_3-O-CH_2-COO^-$) were analyzed by an ion chromatograph equipped with a conductivity detector (specific separation conditions are described in the Supporting Information).

RESULTS AND DISCUSSION

Degradation of PFECAs. *Different Degradability between PFECAs and Traditional PFCAs.* Figure 2 shows the decay and defluorination of four PFASs representing full-carbon-chain PFCAs, linear PFECAs, and branched PFECAs.

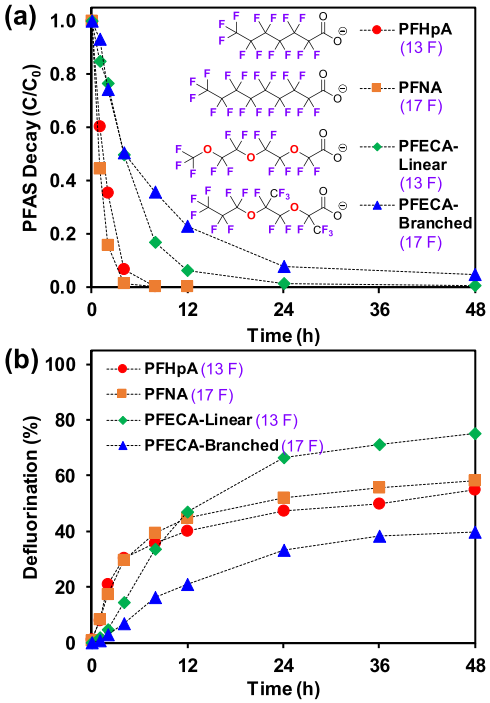

Figure 2. Time profiles for (a) parent compound decay and (b) defluorination percentages for two full-carbon-chain PFCAs with 13 and 17 F atoms, a linear PFECA with 13 F atoms, and a branched PFECA with 17 F atoms. Reaction conditions: PFAS (0.025 mM), Na_2SO_3 (10 mM), carbonate buffer (5 mM), 254 nm irradiation (a 18 W low-pressure Hg lamp for 600 mL solution) at pH 9.5 and 20 °C.

The parent compound decay is the fastest for the two traditional PFCAs and the slowest for the branched PFECA (Figure 2a). The order of parent compound decay rates for these structures does not match the order of their defluorination percentages. Figure 2b shows the distinct defluorination profiles between PFECAs and traditional PFCAs as well as between linear and branched PFECAs. All four PFASs showed an initial period of rapid F^- release, followed by slower F^- release before reaching a plateau. However, the initial rates of defluorination from the two PFECAs are slower than those from the two PFCAs. In particular, the linear PFECA showed a slower initial rate but a significantly deeper defluorination than perfluoroheptanoic acid (i.e., 75 vs 55% of the 13 F atoms in each molecule). In contrast, the branched PFECA showed both a slower rate and a lower extent of defluorination than perfluorononanoic acid (i.e., 40 vs 58% of the 17 F atoms in each molecule). These results suggest new structure−reactivity relationships governing PFECA degradation. To systematically understand these mechanisms, we extended our study to 10 individual PFECAs, which exhibited structure-specific profiles of parent compound decay and defluorination (Table 1 and Figure 3).

Different Degradability of Four PFECA Structure Categories. Category **A** includes structures **A1**−**A3** with branched $-CF_3$ groups, which are the acid forms of hexafluoropropylene oxide dimer, trimer, and tetramer (HFPO−DA, HFPO−TrA, and HFPO−TeA), respectively. The initial rates of parent compound decay were similar (Figure 3a), but longer structures showed a lower deF % (Figure 3b). The defluorination percentages of these branched PFECAs (31−45%) were significantly lower than those of traditional PFCAs (~55%) under the same reaction conditions.[40] Category **B** includes monoether structures **B1**−**B3** with the CF_3O- head group and linear $-(CF_2)_n-$ moieties (n = 1, 2, and 3, respectively) before the terminal $-COO^-$ group. The decay of **B2** and **B3** finished within 12 h (Figure 3c), and the time profiles for their parent compound decay were similar to full-carbon-chain PFCAs (Figure 2a).[40] The final defluorination percentages are also similar (61 and 52% for **B2** and **B3**, respectively, vs 55% for PFCAs). In stark contrast, whereas the decay of **B1** (n = 1) was much slower than those of **B2** and **B3**, the deF % was substantially higher (91%). From the kinetic data, it seems that these $CF_3-O-(CF_2)_n-COO^-$ structures behave similarly to $F(CF_2)_n-COO^-$ under reductive treatment. In our previous study,[40] the decay of CF_3-COO^- took 24 h to complete while the deF % was almost 100%, whereas the decay of all longer PFCAs took 8−12 h to complete, but the maximal deF % was ~55% (Table 1, entry **E1** vs **E2**).

We further tested two linear multiether PFECA categories, **C** and **D**. Both categories contain tetrafluoroethylene oxide (TFEO) building blocks, but the head groups are CF_3O- and C_4F_9O-, respectively. With $-O-CF_2-COO^-$ as the end group, the parent compound decay became slow again (cf. Figure 3e,g). Like the decay profile for the long-molecule **A3** (Figure 3a), the decay of the long-molecule **D2** was also incomplete within 48 h. The other three structures **C1**, **C2**, and **D1** showed profiles similar to the decay of **B1**. The notable difference between these two PFECA categories is that **C1** and **C2** with their short CF_3O- head groups yielded a significantly higher deF % (82 and 75%, respectively) than **D1** and **D2** with their long C_4F_9O- head groups (58 and 65%, respectively) (cf. Figure 3f vs 3h).

https://dx.doi.org/10.1021/acs.est.9b05869
Environ. Sci. Technol. 2020, 54, 2489−2499

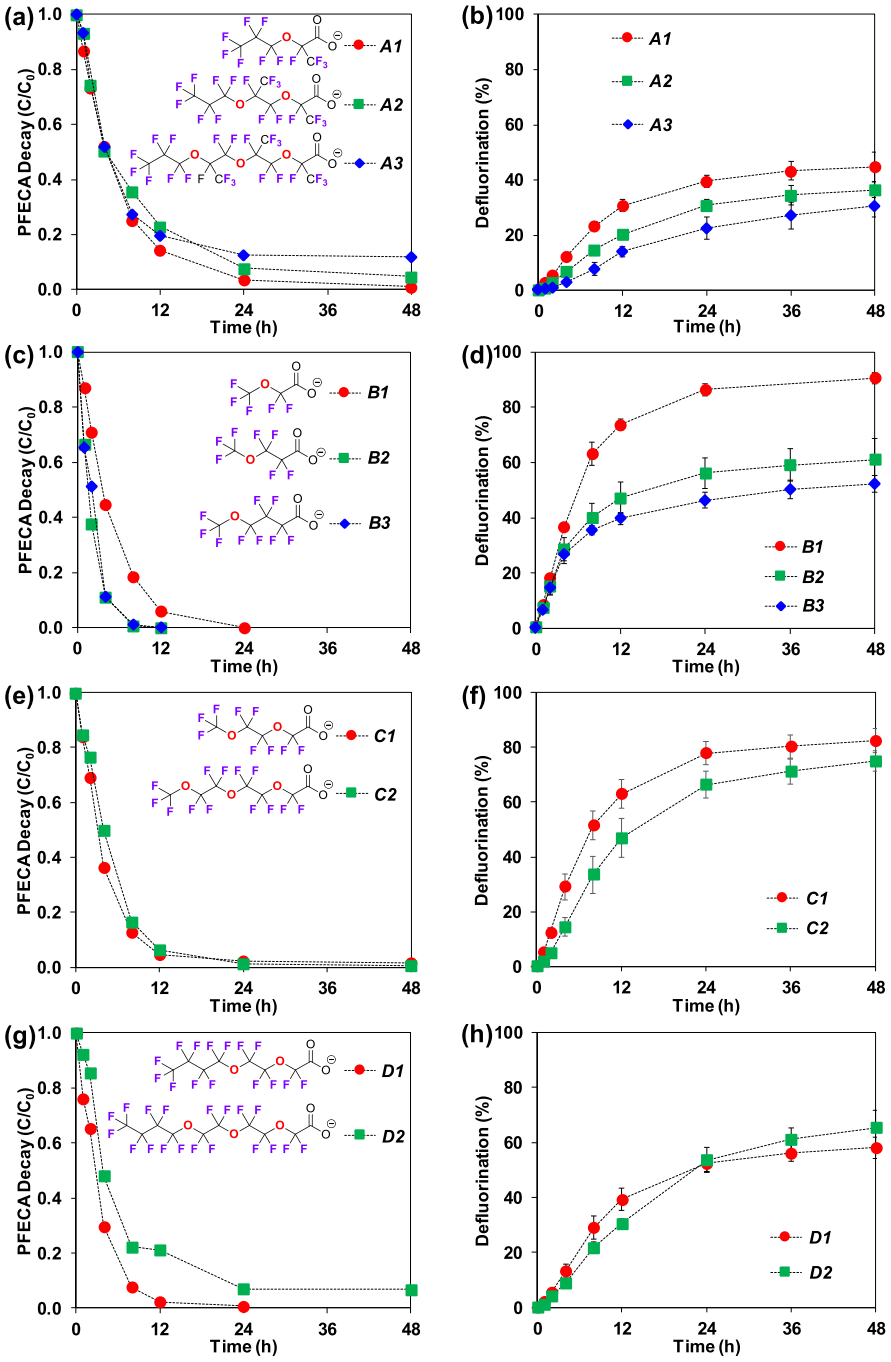

Figure 3. Time profiles of parent compound decay and defluorination for the four PFECA structure categories. Reaction conditions are described in the title of Figure 2.

Structural Effects on PFECA Degradation. The kinetic data shown above indicates the following characteristics of PFECA degradation in comparison to traditional PFCAs: (1) branched PFECAs show slower decay and lower defluorination; (2) linear PFECAs exhibit slower decay if they contain $-O-CF_2-COO^-$ end groups or a very similar rate of decay if more than one $-CF_2-$ linker is present in the $-O-(CF_2)_n-COO^-$ functional group; (3) linear PFECAs containing shorter oxygen-segregated fluoroalkyl moieties showed a higher deF %. To interpret these interesting results on the molecular level, we conducted theoretical calculations and TP analyses.

Theoretical Calculations of C−F and C−O BDEs. The bond dissociation energies (BDEs) of C−F and ether C−O bonds in all PFECA structures were calculated with density functional theory. Representative results are shown in Figure 4, and the full data sets are collected in Figures S2−S5. We identified new trends for C−F BDEs in PFECAs compared to full-carbon-chain PFCAs. First, the ether oxygen increases the BDE of C−F on the adjacent fluorocarbons. While the terminal $-CF_3$ in long fluoroalkyl chains has a typical C−F BDE < 119 kcal mol^{-1} (Figure 4d,f,h,i), the inclusion of ether oxygen atoms increased the C−F BDE to 120−123 kcal mol^{-1} (Figure 4a−c,g). In fluorinated molecules, the ether oxygen acts as an electron-donating group like the $-CH_2-$ group in FTCAs (Figure 4e). With multiple oxygen atoms in the chain, the relatively weak C−F bonds in long-chain PFCAs were not

https://dx.doi.org/10.1021/acs.est.9b05869
Environ. Sci. Technol. 2020, 54, 2489−2499

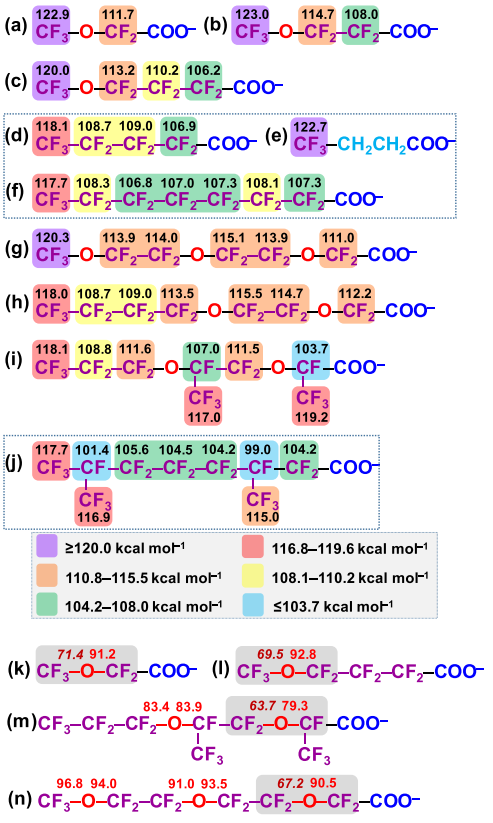

Figure 4. Calculated C−F BDEs (a−j) and C−O BDEs (k−n) (in kcal mol^{-1}) of selected PFASs at the B3LYP-D3(BJ)/6-311+G-(2d,2p) level of theory. Results for all PFECA structures are collected in Figures S2−S5. Data for (d−f,j) are from refs 40 and 41.

found in linear PFECAs (cf. Figure 4f vs 4g,h). In particular, the typically weak C−F bond at the α-position of PFCAs (i.e., BDE < 108 kcal mol^{-1}, Figure 4d,f) does not exist in linear PFECAs with an ether oxygen at the β-position (i.e., $\mathbf{R_F}$−O−CF_2−COO^-, BDE > 111 kcal mol^{-1}, Figure 4a,g,h). However, when the fluoroalkyl chain adjacent to $-COO^-$ is longer (i.e., n = 2 or 3 in $\mathbf{R_F}$−O−$(CF_2)_n$−COO^-), the weak C−F bond at the α-position appears again (Figure 4b,c). These novel trends on C−F BDEs in linear PFECAs corroborate the different rates of parent compound decay. The two structures with the weak α-position C−F bonds (**B2** and **B3** in Figure 3c) showed a rate of decay similar to the full-carbon-chain PFCAs (Figure 2a), whereas the other $\mathbf{R_F}$−O−CF_2−COO^- structures showed slower parent compound decay (**B1**, **C1**, and **C2** in Figure 3c,e).

As for the branched PFECAs, the inclusion of ether oxygen atoms showed a similar effect on increasing the C−F BDEs. In comparison to a full-carbon-chain branched PFCA that contains very weak tertiary C−F bonds,[41] the oxygen atoms in HFPO−TrA significantly strengthen all secondary and tertiary C−F bonds (cf. Figure 4i vs 4j). Although the HFPO oligomer acids contain distinctly weak tertiary C−F bonds (i.e., BDE < 104 kcal mol^{-1}), the rates of the parent compound decay were slower than those of most of the linear PFECAs (Figure 3). Thus, other mechanisms and considerations beyond the cleavage of weak C−F bonds are likely responsible for the degradation of branched PFECAs.

As the cleavage of ether C−O bonds has been proposed for the degradation of HFPO−DA,[38,39] we further examined the BDEs of C−O bonds in all PFECAs. A very interesting phenomenon is the "asymmetric" strength of the two C−O bonds on the first ether linkage counted from the terminal $-COO^-$ (Figure 4k−n). On this ether oxygen atom, the C−O bond away from $-COO^-$ has a considerably lower BDE (63−73 kcal mol^{-1}) than the other one closer to $-COO^-$ (78−94 kcal mol^{-1}). This phenomenon was observed in all PFECAs regardless of the total number of ether linkages, branched versus linear molecular backbone, or the distance between $-COO^-$ and the first ether linkage (cf. Figure 4k vs 4l). The BDE difference between those two C−O bonds in the three branched PFECAs ranges from 14.7 to 18.3 kcal mol^{-1}, and the difference in linear PFECAs is even greater, from 19.8 to 23.3 kcal mol^{-1} (see Figures S2−S5 for full data sets). However, if the PFECA molecule contains multiple ether oxygens, the pairs of C−O bonds in the remaining ether linkages have similar BDEs (i.e., only with small differences ranging from 0.1 to 3.4 kcal mol^{-1}, Figure 4m,n). In addition, because of the electron-withdrawing effect by the $-CF_3$ branches, the BDEs of these "normal" C−O bonds in branched multiether structures (82−84 kcal mol^{-1}) are lower than those in linear multiether structures (89−97 kcal mol^{-1}).

Spontaneous Bond Cleavage in Electron-Added PFECA Radical Anion Structures. The distinctly weak C−O bond in all PFECAs and the relatively weak tertiary C−F bonds in branched PFECAs imply the potential cleavage of these bonds during the reaction. To verify this hypothesis, we further conducted geometry optimization of the radical anion $[\mathbf{R_F}-COO]^{\bullet 2-}$ upon adding an extra electron (which simulates an e_{aq}^-) to the original PFECA anion ($\mathbf{R_F}-COO^-$).[40] As expected, the spontaneous stretching of the α-position C−F bonds (Figure 5a,b) and ether C−O bonds (Figure 5c,d) was

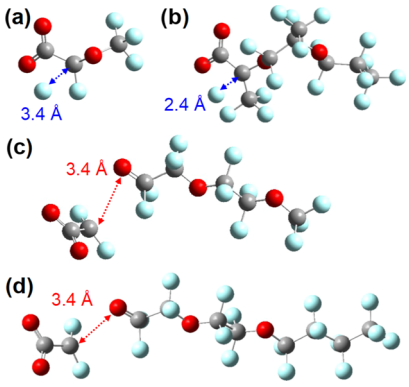

Figure 5. Geometry-optimized structure of the adducts of PFECA anions with an e_{aq}^- ($PFECA^{\bullet 2-}$) at the B3LYP-D3(BJ)/6-311+G-(2d,2p) level of theory, showing the stretching of C−F (blue) and C−O (red) bonds. Results for all PFECA structures are collected in Figures S6 and S7.

observed. The distance between the two atoms stretched considerably longer than the normal length for C−O and C−F bonds (i.e., bond cleavage). The results for all PFECA structures are collected in Figures S6 and S7.

Interestingly, although the calculated C−O bond cleavage in $[\mathbf{R_F}-COO]^{\bullet 2-}$ structures indeed occurred at the first ether linkage counted from the $-COO^-$ group, the cleaved C−O bond was not the "significantly weaker one" as calculated in the original $\mathbf{R_F}-COO^-$ (e.g., Figure 5c vs 4n). This discrepancy could be due to the addition of the extra electron, which altered the bonding structure of PFECA anions. More

https://dx.doi.org/10.1021/acs.est.9b05869
Environ. Sci. Technol. 2020, 54, 2489−2499

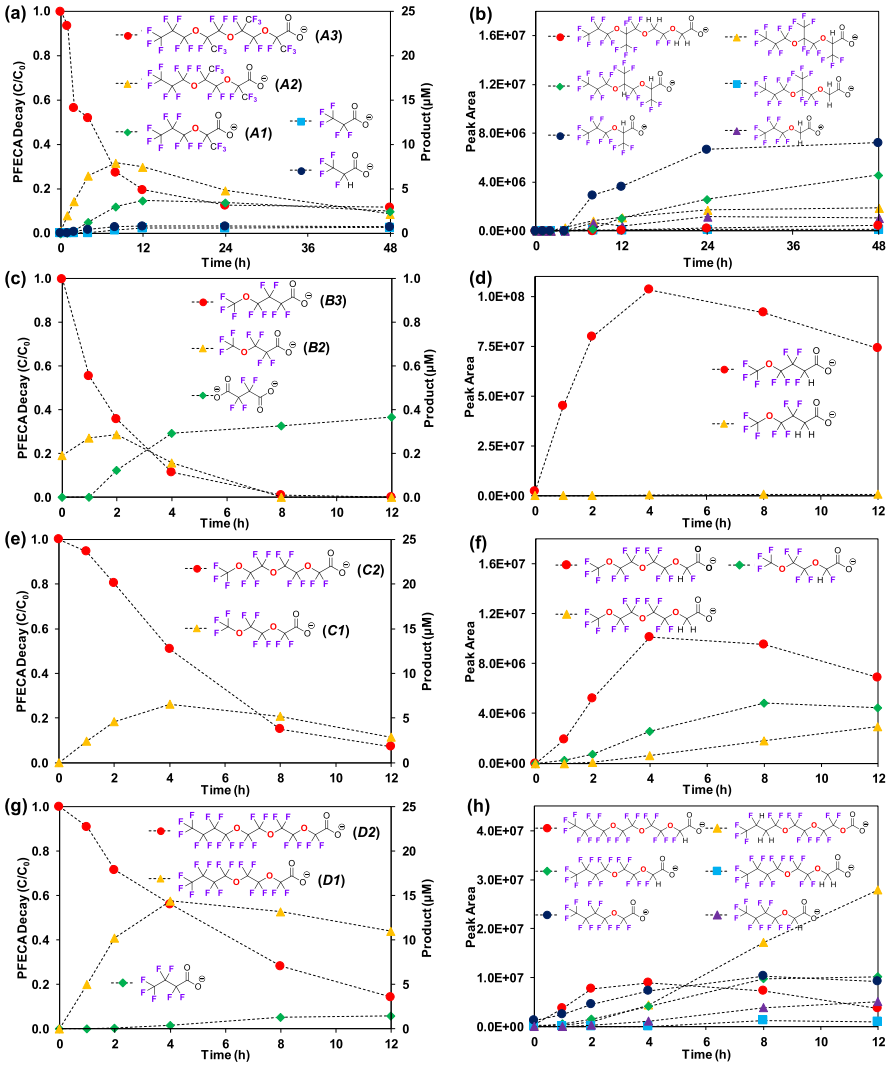

Figure 6. Representative degradation products of the longest compound in each structure category (**A3**, **B2**, **C2**, and **D2**, C_0 = 25 μM). Reaction conditions are described in the title of Figure 2. For each structure, quantified products with standard compounds are shown in the left panel, and species without standard compounds are presented in peak areas in the right panel. All detected species are listed in Tables S1−S9.

importantly, the calculation shows that C−O bond cleavage can be a major pathway for PFECA degradation by e_{aq}^-. The previously elucidated cleavage of weak C−F bonds[40] was also observed both from branched PFECAs (with very weak tertiary C−F bonds) and from the linear structure **B1** CF_3−O−CF_2−COO^- where the α-position C−F BDE is relatively high (112 kcal mol^{-1}). These results suggest that C−F bond cleavage can be another degradation pathway, even if the inclusion of ether oxygen atoms causes many C−F bonds to be more recalcitrant than those in full-carbon-chain PFCAs.

PFECA Degradation Product Analysis. The above theoretical calculations have indicated the possibility of C−F and C−O bond cleavage. On the basis of our previous study, the decarboxylation−hydroxylation−HF elimination−hydrolysis (DHEH) is another major degradation pathway for structures with the fluoroalkyl moiety directly linked with $-COO^-$.[40] Hence, we hypothesized that the degradation of PFECAs takes place via at least three pathways: (i) cleavage of weak C−F bonds and the formation of C−H bonds (i.e., H/F exchange), (ii) DHEH, and (iii) characteristic cleavage of ether C−O bonds. To detect the TPs and confirm the degradation pathways, we used both targeted analysis with triple quadruple mass spectrometry and suspect screening with high-resolution mass spectrometry data (all results are collected in Tables S1−S9). A series of TPs was detected, which supports all three proposed degradation pathways. The overall TP detection and the corresponding degradation pathways from the longest PFECA in each of the four structure categories are discussed below (Figure 6, and Schemes 1 and 2). The reaction schemes proposed for individual PFECAs are provided in Schemes S1−S10.

As shown in Figure 6a, the degradation of **A3** HFPO−TeA generated **A2** HFPO−TrA and **A1** HFPO−DA daughter products. The maximum concentrations of **A2** (7.9 μM) and **A1** (3.7 μM) were detected at 8 and 12 h, respectively. We attribute this transformation to the cleavage of the first C−O bond counted from the terminal $-COO^-$ group. The two fragments reacted with H_2O to form two perfluorinated alcohols, which were not stable and subject to HF elimination to acyl fluoride.[42,43] The subsequent hydrolysis generated carboxylic acid, resulting in the net conversion from $\mathbf{R_F}$−CF_2OH into $\mathbf{R_F}$−COO^- and two F^- ions. The C−O cleavage on the first ether linkage counted from $-COO^-$ shortens HFPO−TeA into HFPO−TrA and then into HFPO−DA,

https://dx.doi.org/10.1021/acs.est.9b05869
Environ. Sci. Technol. 2020, 54, 2489−2499

Scheme 1. Degradation Pathways for (a) HFPO Oligomer Acids Starting from the Longest Compound A3 and (b) the Daughter Product PFPrA; Detected TPs are Highlighted

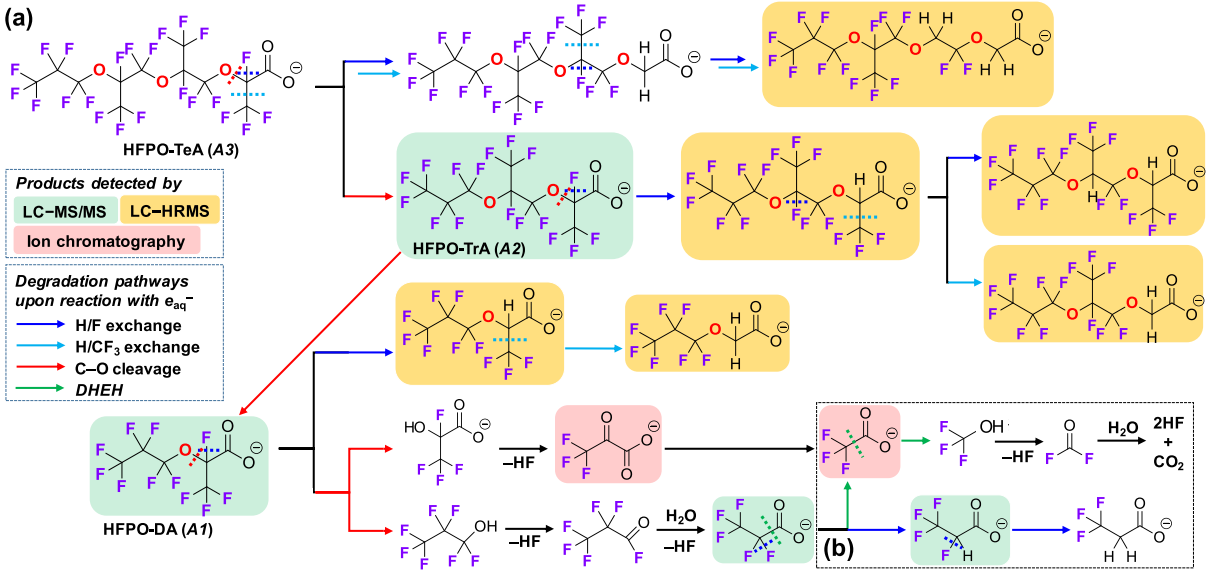

Scheme 2. Degradation Pathways for the Three PFECA Structure Categories Starting from the Longest Compound (a) B3, (b) C2, and (c) D2; Detected TPs are Highlighted

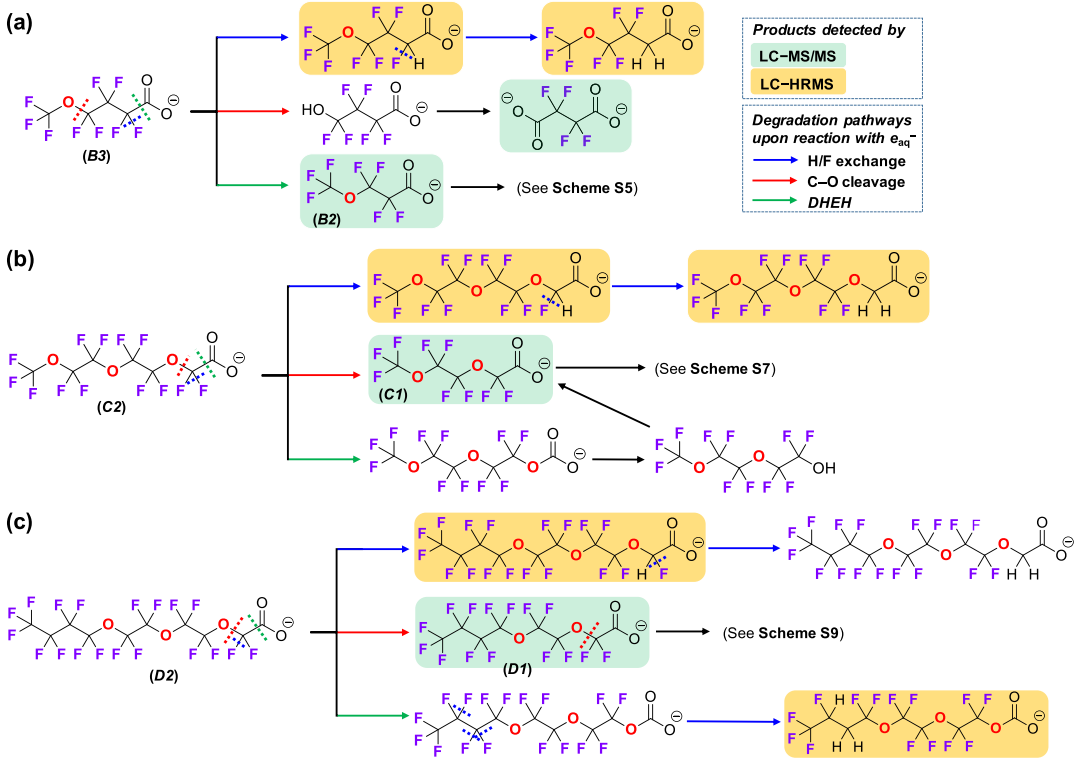

which can be further degraded into $CF_3CF_2–COO^-$ via another C–O cleavage (Scheme 1). Each round of C–O cleavage also generated the same product $CF_3CF(OH)–COO^-$, which underwent further HF elimination into $CF_3–CO–COO^-$ (TFPy), as structures with F and OH on the same carbon (e.g., FCH_2OH) are generally unstable.[44] We confirmed the formation of TFPy during the degradation of HFPO–DA with IC detection (Figure S8). Like $CF_3–COO^-$ (trifluoroacetic acid, TFA), pure TFPy also showed near-complete defluorination (Figure S9), and TFA is a possible degradation intermediate (Figure S10). Although TFA was not detected in our samples from HFPO–DA degradation, we have elucidated that TFA can be generated from both $CF_3CF_2–COO^-$ and TFPy and then completely mineralized via the DHEH pathway (Scheme 1b).[40]

Suspect screening using the HRMS data identified a series of H/F exchange products from the HFPO oligomer acids. On the basis of our calculations, we assign the C–H bonds to the branched carbons (particularly the α-position branched carbon) where weak tertiary C–F bonds are located (Figure

https://dx.doi.org/10.1021/acs.est.9b05869
Environ. Sci. Technol. 2020, 54, 2489–2499

6b and Scheme 1a). We also observed products missing one or more $-CF_3$ groups (i.e., H/CF_3 exchange). By comparing the results with those for linear PFECAs, such TP structures missing $-CF_3$ groups are specific for branched PFECAs. Therefore, we interpret the transformation pathway to be the cleavage of the branching $-CF_3$ rather than the terminal $-CF_3$. In addition, the degradation products and reaction schemes from pure HFPO–DA and HFPO–TrA (Tables S1 and S2 and Schemes S1 and S2) further corroborate the mechanistic insights obtained from HFPO–TeA degradation.

For the degradation of **B3** (CF_3–O–$CF_2CF_2CF_2$–COO^-), the C–O bond cleavage mechanism was confirmed by the detection of ^-OOC–CF_2CF_2–COO^- (Figure 6c and Scheme 2a). The head CF_3– group was thus believed to be fully defluorinated via the formation of unstable CF_3–OH. The DHEH mechanism was also confirmed by the generation of **B2** CF_3–O–CF_2CF_2–COO^-. The HRMS detection of two products with one and two H/F exchanges on the parent compound (most probably at the α-position) is not surprising (Figure 6d).

The degradation of the two multiether linear PFECAs **C2** and **D2** also followed the three reaction pathways, which are supported by the TPs identified (Figure 6e–h). Although the C–F BDEs of the α-position $-CF_2-$ in these structures are higher than those in full-carbon-chain PFCAs (Figure 4g vs 4f), the H/F-exchanged TPs were detected, thus corroborating the spontaneous C–F bond stretching by theoretical calculations (Figure 5a).

Additionally, the C–O bond cleavage in **B1** (also in category **C** and **D** structures that contain $-O-CF_2-COO^-$) was supposed to generate $HO-CF_2-COO^-$, which should further decompose into oxalate ($^-OOC-COO^-$). IC detection confirmed the formation of oxalate (Figure S11), thus further consolidating this C–O bond cleavage mechanism.

Overall Mechanistic Insights into Reductive PFECA Degradation. On the basis of the degradation kinetics, theoretical calculations, and TP analyses, we have confirmed that the PFECAs have three pathways for the reductive degradation by e_{aq}^-: (1) ether C–O bond cleavage, (2) C–C bond cleavage, including the decarboxylation step of DHEH and the cleavage of $-CF_3$ from branched PFECAs, and (3) direct C–F bond cleavage followed by H/F exchange. Here, we categorize the first two as indirect pathways for defluorination and the third one as a direct pathway for defluorination. It is worth noting here that all three independent pathways are enabled upon PFECAs interacting with e_{aq}^-. First, control experiments with UV irradiation without adding sulfite showed very slow and limited degradation (Figure S12). Second, spontaneous C–O bond cleavage was observed after the PFECA anion received an extra electron (Figure 5). Third, the generation of e_{aq}^- from sulfite has been confirmed by spectroscopic observations,[45,46] and other chemicals such as iodide[47] and indole[48] have also been used as the source of e_{aq}^-, which have achieved similar results for PFOA defluorination.

The cleavage of the C–O or C–C bond in PFECAs will generate perfluoroalcohols, which will undergo HF elimination and the following hydrolysis to yield two F^- and the corresponding carboxylic acids. This mechanism has been collectively supported by (1) the decay of HFPO and TFEO oligomer acids into shorter analogues (Figure 6a,e,g, supporting C–O cleavage) and the decay of **B3** into **B2** (Figure 6c, supporting C–C cleavage), (2) the generation of $^-OOC-CF_2CF_2-COO^-$ from **B3** (CF_3–O–$CF_2CF_2CF_2$–COO^-) and the generation of $^-OOC-COO^-$ from R_F–O–CF_2–COO^- structures, and most importantly (3) the high deF % of linear PFECAs with short oxygen-segregated fluorocarbon moieties. The results in Figure 3d,f,h show a clear trend that PFECAs containing longer fluorocarbon moieties (rather than a longer length of the molecule) yielded a lower deF %. Because the perfluoroalcohol decomposition can only ensure the liberation of two F^- ions, if this step yields a full-carbon-chain PFCA containing two or more fluorocarbons, a relatively easy H/F exchange on the α-position will occur, yielding R_F–CH_2–COO^-. As previously elucidated, the reductive defluorination of this product is very sluggish, especially when the R_F moiety is short (i.e., lack of weak C–F bonds).[40]

Among all PFECAs, **B1** (CF_3–O–CF_2–COO^-) allowed an outstanding deF % at 91% because either C–O cleavage or decarboxylation will trigger the perfluoroalcohol decomposition mechanism to liberate all five F^- ions from the two oxygen-segregated single fluorocarbons. We hypothesized that the incomplete defluorination was attributed to the minor chance of H/F exchange on the α-position (Figure 5a). To verify this hypothesis, we examined the degradation of polyfluorinated CF_3–O–CH_2–COO^- under the same reaction conditions (Figure 7). As expected, the $-CH_2-$ group at

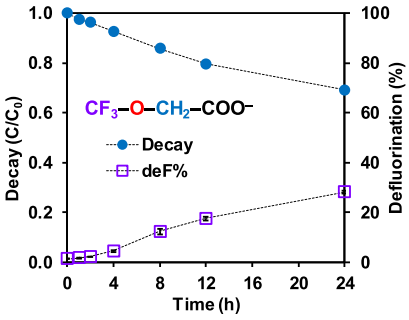

Figure 7. Time profiles of parent compound decay and defluorination for polyfluorinated CF_3–O–CH_2–**COO**$^-$ under the same reaction conditions for all other PFECAs (described in the title of Figure 2).

the α-position leads to a high recalcitrance in comparison with **B1** (Figure 3c,d). However, to our surprise, the degradation at 24 h (30%) was much higher than the full-carbon-chain counterpart CF_3CH_2–COO^- (<2%).[40] The overall deF % of 28% indicates near-complete defluorination of the decayed 30% fraction of the parent compound, and the time profiles of the parent compound decay and defluorination are highly symmetric. These results support the degradation mechanism of C–O bond cleavage rather than a stepwise H/F exchange. Therefore, C–O bond cleavage can still occur in a polyfluorinated ether structure, with a hydrocarbon moiety segregating the $-COO^-$ group from the fluorinated moiety. The rate is faster than in a polyfluorinated full-carbon-chain structure but slower than in a perfluorinated ether structure.

For comparison, under the same reaction conditions, the deF % for the full-carbon CF_3CF_2–COO^- was 53%.[40] In our previous study, by assuming that CF_3CF_2–COO^- will take either H/F exchange (forming the highly recalcitrant CF_3CH_2–COO^- with negligible further degradation, with an overall deF % of 40%) or DHEH (leading to 100% defluorination via forming CF_3–COO^-), we estimated that the probability of CF_3CF_2–COO^- undergoing the H/F exchange versus DHEH is 75 versus 25%.[40] Similarly, if all

https://dx.doi.org/10.1021/acs.est.9b05869
Environ. Sci. Technol. 2020, 54, 2489–2499

B1 $CF_3-O-CF_2-COO^-$ first undergoes C−O or C−C bond cleavage, 100% defluorination would be achieved. If all **B1** first undergoes H/F exchange to yield $CF_3-O-CH_2-COO^-$ (deF % = 40% at this step), which then undergoes slow degradation for up to 30%, this would result in 40% + 60% × 30% = 58% defluorination. Hence, to yield an overall defluorination of 91% through the two competing pathways, the probability for **B1** to undergo H/F exchange is only 21%. This significantly decreased probability of H/F exchange from 75 to 21% should be attributed to the increased α-position C−F BDE in the $R_F-O-CF_2-COO^-$ structures (Figure 4a,g,h). This mechanistic insight also explains the low deF % for **B2** $CF_3-O-CF_2CF_2-COO^-$ and **B3** $CF_3-O-CF_2CF_2CF_2-COO^-$, as the lower α-position C−F BDEs (Figure 4b,c) enabled easier H/F exchange. In Figure 3, the parent compound decays of **B2** and **B3** were faster than those of all $R_F-O-CF_2-COO^-$ compounds. The formation of $-CH_2-$ at the α-position significantly slowed down further degradation. In contrast, all PFECAs that allowed higher deF % than PFCAs (~55%)[40] contain only short (**C1** or **C2**) fluorocarbon moieties, which suppress the direct defluorination via H/F exchange (an unfavorable pathway, typically breaking weak C−F bonds) and enhance the indirect defluorination via C−O or C−C bond cleavage (a favorable pathway, breaking all C−F bonds on the carbon bearing −OH, regardless of the BDEs).

The above mechanistic insights also explain the degradation pattern of branched PFECAs. The branching $-CF_3$ generates distinctly weak tertiary C−F bonds, especially at the α-position (Figures 4i and S2). As shown in Figures 5b and 6b, these structures have a high tendency to undergo H/F exchange. The following cleavage of the branching $-CF_3$ leads to the formation of $-CH_2-$ at the α-position, thus retarding further degradation. The longest structure **A3** has three tertiary C−F bonds; thus, the parent **A3** and the C−O cleavage products **A2** and **A1** all have a high probability of an unfavorable H/F exchange. Therefore, **A3** showed the lowest deF % among the three branched PFECAs. From the HRMS data for all PFECAs (Tables S1−S9), in general, the TPs with one H/F exchange increased at the beginning of the reaction and then slowly decreased. In contrast, the two H/F exchange TPs slowly accumulated throughout the reaction, indicating high recalcitrance. In comparison to linear PFECAs and full-carbon-chain PFCAs, the slower parent compound decay of branched PFECAs is probably attributed to the kinetic hindrance by the branching $-CF_3$.

We note that earlier studies by Bao et al.[38,39] on the degradation of HFPO oligomer acids (**A1**, **A2**, and **A3**) observed a significantly faster parent compound decay and higher deF % than our observations. In comparison to our reaction settings (one UV lamp for a 600 mL solution, pH 9.5, and 10 mM sulfite), Bao et al. used considerably more favorable conditions, including intense UV irradiation (16 similar UV lamps for a 45 mL solution), tripled basicity (pH 10), and a doubled sulfite concentration (20 mM). Because the duplication of using 20 mM sulfite at pH 10 in our photoreactors (one UV lamp for a 600 mL solution) achieved limited improvements on deF % (Figure S13), the significantly higher defluorination observed by Bao et al.[38,39] should be attributed to the higher intensity of the 254 nm UV irradiation. Nonetheless, by comparing all PFECA compounds, we have identified new structural features allowing much deeper defluorination than HFPO oligomers. We expect that further enhanced degradation of PFECA structures can be achieved under energy−efficient reaction conditions, which are under optimization in our lab.

Implications for Fluorochemical Design and Environmental Remediation. As seen from the diverse PFECA structures involved in this study, the design of PFECA is highly flexible as multiple fluorinated building blocks can be integrated into the molecule in various sequences. Although the design rationale of individual PFECAs (e.g., branched vs linear and the length of oxygen-segregated fluorocarbon moieties) and their targeted properties for specific industrial applications remain largely unknown to the environmental chemistry community, we are able to identify critical molecular features that can lead to enhanced PFECA degradation using reductive approaches. UV irradiation (on sulfite, iodide, indole, or hydroxyl radical scavengers),[46−49] plasma treatment,[34] and high-energy irradiation[33] all involve e_{aq}^- as a primary reactive species. In general, the switch from full-carbon-chain PFCAs to PFECAs has indeed brought in unique advantages that enable deeper defluorination, including (1) spontaneous defluorination from alcohol intermediates upon C−O cleavage and (2) suppressed H/F exchange due to the strong C−F bonds. To minimize the incomplete defluorination caused by the conversion into recalcitrant products (e.g., with $-CH_2-$ separating the fluoroalkyl moiety and $-COO^-$), a desirable structural feature is $R_F-O-CF_2-COO^-$. In other words, the last building block of the PFECA molecule can be a TFEO; after the epoxide ring opens, the alcohol product $R_F-O-CF_2CF_2OH$ will transform to $R_F-O-CF_2-COO^-$. As elucidated in earlier sections, the relatively high BDE of the α-position C−F favors indirect defluorination through C−O cleavage and decarboxylation. The other desirable structural feature is to limit the length of other fluorocarbon moieties segregated by ether oxygen atoms. If the chain length is **C1** (either CF_3-O- or $-O-CF_2-O-$), the C−O cleavage is expected to provide complete defluorination of that fluorocarbon moiety. This prediction, which is based on model PFECAs studied in this work, can be further examined when chemicals containing $-O-CF_2-O-$ moieties [e.g., $CF_3-(O-CF_2)_n-O-CF_2-COO^-$, n = 1 to 3][24,27] become available for experimental tests. Because the oxygen atoms substantially increase C−F BDEs (Figure 4), direct H/F exchange on **C1** or **C2** fluorocarbon moieties (not linked with $-COO^-$) is less likely. However, for **C2** fluorocarbon moieties (e.g., $-O-CF_2CF_2-O-$), the formation of $-O-CF_2-COO^-$ will still induce a low probability of H/F exchange.

On the other hand, the mechanistic insights from this study will guide the development of PFECA degradation technologies. In particular, if direct defluorination cannot be fully avoided, effective degradation of the recalcitrant polyfluorinated products will be necessary to ensure deep or complete defluorination. Although we observed poor defluorination from the branched PFECAs that contain very weak tertiary C−F bonds and a long C3 fluorocarbon moiety, studies by Bao et al.[38,39] have achieved deep defluorination of those structures by applying a high UV intensity. Therefore, coordinated efforts from both fluorochemical design (e.g., developing PFECAs with high degradability) and environmental remediation (e.g., optimizing the consumption of energy and chemicals) can be expected to transform the development, use, and treatment of fluorinated chemicals, with minimal adverse impact on the environment.

https://dx.doi.org/10.1021/acs.est.9b05869
Environ. Sci. Technol. 2020, 54, 2489−2499

■ ASSOCIATED CONTENT

Supporting Information

The Supporting Information is available free of charge at https://pubs.acs.org/doi/10.1021/acs.est.9b05869.

Detailed experimental procedures; LC−MS data; calculation results; ion-chromatography analyses of small ionic TPs; additional kinetics data; and proposed PFECA degradation mechanisms (PDF)

■ AUTHOR INFORMATION

Corresponding Author

Jinyong Liu − *Department of Chemical & Environmental Engineering, University of California, Riverside, Riverside, California 92521, United States;* orcid.org/0000-0003-1473-5377; Email: jyliu@engr.ucr.edu, jinyong.liu101@gmail.com

Authors

Michael J. Bentel − *Department of Chemical & Environmental Engineering, University of California, Riverside, Riverside, California 92521, United States;* orcid.org/0000-0003-1404-113X

Yaochun Yu − *Department of Civil & Environmental Engineering, University of Illinois at Urbana−Champaign, Urbana, Illinois 61801, United States;* orcid.org/0000-0001-9231-6026

Lihua Xu − *Department of Chemical & Environmental Engineering, University of California, Riverside, Riverside, California 92521, United States*

Hyuna Kwon − *Department of Chemical & Environmental Engineering, University of California, Riverside, Riverside, California 92521, United States*

Zhong Li − *Metabolomics Lab of Roy J. Carver Biotechnology Center, University of Illinois at Urbana−Champaign, Urbana, Illinois 61801, United States*

Bryan M. Wong − *Department of Chemical & Environmental Engineering and Materials Science & Engineering Program, University of California, Riverside, Riverside, California 92521, United States;* orcid.org/0000-0002-3477-8043

Yujie Men − *Department of Chemical & Environmental Engineering, University of California, Riverside, Riverside, California 92521, United States; Department of Civil & Environmental Engineering and Institute for Genomic Biology, University of Illinois at Urbana−Champaign, Urbana, Illinois 61801, United States;* orcid.org/0000-0001-9811-3828

Complete contact information is available at: https://pubs.acs.org/10.1021/acs.est.9b05869

Notes

The authors declare no competing financial interest.

■ ACKNOWLEDGMENTS

Financial support was provided by the UCR Initial Complement for J.L., the UCR Collaborative Seed Grant for J.L., B.M.W., L.X., and H.K., the National Science Foundation (CHE-1709719 for J.L. and CHE-1709286 for Y.M. and Y.Y.), and the Strategic Environmental Research and Development Program (ER-1289 for J.L., M.J.B., and B.M.W.). M.J.B. also received a scholarship from the UCR Water SENSE Integrative Graduate Education and Research Traineeship (IGERT) supported by the NSF. UCR undergraduate researchers Andrew Dalmacio, Duy Dao, Maggy Harake, Vivian Ngo, and Wenxiaoshan Sui provided technical assistance on photochemical reactions. We also thank Dr. Mark Strynar for kindly providing compound **B1**.

■ REFERENCES

(1) Banks, R. E.; Smart, B. E.; Tatlow, J. *Organofluorine Chemistry: Principles and Commercial Applications*; Springer Science & Business Media, 2013.

(2) Wang, Z.; DeWitt, J. C.; Higgins, C. P.; Cousins, I. T. A never-ending story of per-and polyfluoroalkyl substances (PFASs)? *Environ. Sci. Technol.* **2017**, *51*, 2508−2518.

(3) Buck, R. C.; Franklin, J.; Berger, U.; Conder, J. M.; Cousins, I. T.; De Voogt, P.; Jensen, A. A.; Kannan, K.; Mabury, S. A.; van Leeuwen, S. P. Perfluoroalkyl and polyfluoroalkyl substances in the environment: terminology, classification, and origins. *Integr. Environ. Assess. Manage.* **2011**, *7*, 513−541.

(4) Meshri, D. T. The modern inorganic fluorochemical industry. *J. Fluorine Chem.* **1986**, *33*, 195−226.

(5) Xiao, F. Emerging poly-and perfluoroalkyl substances in the aquatic environment: a review of current literature. *Water Res.* **2017**, *124*, 482−495.

(6) Liu, J.; Mejia Avendaño, S. Microbial degradation of polyfluoroalkyl chemicals in the environment: A review. *Environ. Int.* **2013**, *61*, 98−114.

(7) Kelly, B. C.; Ikonomou, M. G.; Blair, J. D.; Surridge, B.; Hoover, D.; Grace, R.; Gobas, F. A. P. C. Perfluoroalkyl contaminants in an Arctic marine food web: trophic magnification and wildlife exposure. *Environ. Sci. Technol.* **2009**, *43*, 4037−4043.

(8) United States Environmental Protection Agency. Revisions to the unregulated contaminant monitoring regulation (UCMR 3) for public water systems. *Fed. Regist.* **2012**, *77*, 26071−26101.

(9) United States Environmental Protection Agency. Lifetime health advisories and health effects support documents for perfluorooctanoic acid and perfluorooctane sulfonate. *Fed. Regist.* **2016**, *81*, 33250−33251.

(10) COMMISSION REGULATION (EU) 2017/1000 of 13 June 2017 amending Annex XVII to Regulation (EC) No. 1907/2006 of the European Parliament and of the Council concerning the Registration, Evaluation, Authorisation and Restriction of Chemicals (REACH) as regards perfluorooctanoic acid (PFOA), its salts and PFOA-related substances. *Off. J. Eur. Union* **2017**, 14.6.2017, L 150/14-L 150/18.

(11) Post, G. B.; Gleason, J. A.; Cooper, K. R. Key scientific issues in developing drinking water guidelines for perfluoroalkyl acids: Contaminants of emerging concern. *PLoS Biol.* **2017**, *15*, No. e2002855.

(12) U.S. EPA. 2010/15 PFOA Stewardship Program. https://www.epa.gov/assessing-and-managing-chemicals-under-tsca/risk-management-and-polyfluoroalkyl-substances-pfass#tab-3 (accessed January 27, 2020).

(13) Wang, J.; Pan, Y.; Cui, Q.; Yao, B.; Wang, J.; Dai, J. Penetration of PFASs across the blood cerebrospinal fluid barrier and its determinants in humans. *Environ. Sci. Technol.* **2018**, *52*, 13553−13561.

(14) Rappazzo, K.; Coffman, E.; Hines, E. Exposure to perfluorinated alkyl substances and health outcomes in children: a systematic review of the epidemiologic literature. *Int. J. Environ. Res. Public Health* **2017**, *14*, 691.

(15) Brandsma, S.; Koekkoek, J.; van Velzen, M.; de Boer, J. The PFOA substitute GenX detected in the environment near a fluoropolymer manufacturing plant in the Netherlands. *Chemosphere* **2019**, *220* (220), 493−500.

(16) Wang, Z.; Cousins, I. T.; Scheringer, M.; Hungerbühler, K. Fluorinated alternatives to long-chain perfluoroalkyl carboxylic acids (PFCAs), perfluoroalkane sulfonic acids (PFSAs) and their potential precursors. *Environ. Int.* **2013**, *60*, 242−248.

(17) Strynar, M.; Dagnino, S.; McMahen, R.; Liang, S.; Lindstrom, A.; Andersen, E.; McMillan, L.; Thurman, M.; Ferrer, I.; Ball, C.

Identification of novel perfluoroalkyl ether carboxylic acids (PFECAs) and sulfonic acids (PFESAs) in natural waters using accurate mass time-of-flight mass spectrometry (TOFMS). *Environ. Sci. Technol.* **2015**, *49*, 11622−11630.
(18) Pan, Y.; Zhang, H.; Cui, Q.; Sheng, N.; Yeung, L. W. Y.; Guo, Y.; Sun, Y.; Dai, J. First report on the occurrence and bioaccumulation of hexafluoropropylene oxide trimer acid: An emerging concern. *Environ. Sci. Technol.* **2017**, *51*, 9553−9560.
(19) Pan, Y.; Zhang, H.; Cui, Q.; Sheng, N.; Yeung, L. W. Y.; Sun, Y.; Guo, Y.; Dai, J. Worldwide distribution of novel perfluoroether carboxylic and sulfonic acids in surface water. *Environ. Sci. Technol.* **2018**, *52*, 7621−7629.
(20) Sun, M.; Arevalo, E.; Strynar, M.; Lindstrom, A.; Richardson, M.; Kearns, B.; Pickett, A.; Smith, C.; Knappe, D. R. U. Legacy and emerging perfluoroalkyl substances are important drinking water contaminants in the Cape Fear River Watershed of North Carolina. *Environ. Sci. Technol. Lett.* **2016**, *3*, 415−419.
(21) Gebbink, W. A.; van Asseldonk, L.; van Leeuwen, S. P. J. Presence of emerging per-and polyfluoroalkyl substances (PFASs) in river and drinking water near a fluorochemical production plant in the Netherlands. *Environ. Sci. Technol.* **2017**, *51*, 11057−11065.
(22) Conley, J. M.; Lambright, C. S.; Evans, N.; Strynar, M. J.; McCord, J.; McIntyre, B. S.; Travlos, G. S.; Cardon, M. C.; Medlock-Kakaley, E.; Hartig, P. C.; Wilson, V. S.; Gray, L. E. Adverse Maternal, Fetal, and Postnatal Effects of Hexafluoropropylene Oxide Dimer Acid (GenX) from Oral Gestational Exposure in Sprague-Dawley Rats. *Environ. Health Perspect.* **2019**, *127*, 037008.
(23) Sheng, N.; Pan, Y.; Guo, Y.; Sun, Y.; Dai, J. Hepatotoxic effects of hexafluoropropylene oxide trimer acid (HFPO-TA), a novel perfluorooctanoic acid (PFOA) alternative, on mice. *Environ. Sci. Technol.* **2018**, *52*, 8005−8015.
(24) Cui, Q.; Pan, Y.; Zhang, H.; Sheng, N.; Wang, J.; Guo, Y.; Dai, J. Occurrence and tissue distribution of novel perfluoroether carboxylic and sulfonic acids and legacy per/polyfluoroalkyl substances in black-spotted frog (Pelophylax nigromaculatus). *Environ. Sci. Technol.* **2018**, *52*, 982−990.
(25) Sheng, N.; Cui, R.; Wang, J.; Guo, Y.; Wang, J.; Dai, J. Cytotoxicity of novel fluorinated alternatives to long-chain perfluoroalkyl substances to human liver cell line and their binding capacity to human liver fatty acid binding protein. *Arch. Toxicol.* **2018**, *92*, 359−369.
(26) Hill, J. T. Polymers from hexafluoropropylene oxide (HFPO). *J. Macromol. Sci., Chem.* **1974**, *8*, 499−520.
(27) McCord, J.; Strynar, M. Identification of per-and polyfluoroalkyl substances in the Cape Fear River by high resolution mass spectrometry and nontargeted screening. *Environ. Sci. Technol.* **2019**, *53*, 4717−4727.
(28) McCord, J.; Newton, S.; Strynar, M. Validation of quantitative measurements and semi-quantitative estimates of emerging perfluoroethercarboxylic acids (PFECAs) and hexfluoroprolyene oxide acids (HFPOAs). *J. Chromatogr. A* **2018**, *1551*, 52−58.
(29) Wang, Y.; Yu, N.; Zhu, X.; Guo, H.; Jiang, J.; Wang, X.; Shi, W.; Wu, J.; Yu, H.; Wei, S. Suspect and nontarget screening of per-and polyfluoroalkyl substances in wastewater from a fluorochemical manufacturing park. *Environ. Sci. Technol.* **2018**, *52*, 11007−11016.
(30) Merino, N.; Qu, Y.; Deeb, R. A.; Hawley, E. L.; Hoffmann, M. R.; Mahendra, S. Degradation and removal methods for perfluoroalkyl and polyfluoroalkyl substances in water. *Environ. Eng. Sci.* **2016**, *33*, 615−649.
(31) Schaefer, C. E.; Andaya, C.; Burant, A.; Condee, C. W.; Urtiaga, A.; Strathmann, T. J.; Higgins, C. P. Electrochemical treatment of perfluorooctanoic acid and perfluorooctane sulfonate: Insights into mechanisms and application to groundwater treatment. *Chem. Eng. J.* **2017**, *317*, 424−432.
(32) Gole, V. L.; Fishgold, A.; Sierra-Alvarez, R.; Deymier, P.; Keswani, M. Treatment of perfluorooctane sulfonic acid (PFOS) using a large-scale sonochemical reactor. *Sep. Purif. Technol.* **2018**, *194*, 104−110.
(33) Zhang, Z.; Chen, J.-J.; Lyu, X.-J.; Yin, H.; Sheng, G.-P. Complete mineralization of perfluorooctanoic acid (PFOA) by γ-irradiation in aqueous solution. *Sci. Rep.* **2015**, *4*, 7418.
(34) Stratton, G. R.; Dai, F.; Bellona, C. L.; Holsen, T. M.; Dickenson, E. R. V.; Mededovic Thagard, S. Plasma-based water treatment: Efficient transformation of perfluoroalkyl substances in prepared solutions and contaminated groundwater. *Environ. Sci. Technol.* **2017**, *51*, 1643−1648.
(35) Trojanowicz, M.; Bojanowska-Czajka, A.; Bartosiewicz, I.; Kulisa, K. Advanced oxidation/reduction processes treatment for aqueous perfluorooctanoate (PFOA) and perfluorooctanesulfonate (PFOS)−A review of recent advances. *Chem. Eng. J.* **2018**, *336*, 170−199.
(36) Hori, H.; Nagano, Y.; Murayama, M.; Koike, K.; Kutsuna, S. Efficient decomposition of perfluoroether carboxylic acids in water with a combination of persulfate oxidant and ultrasonic irradiation. *J. Fluorine Chem.* **2012**, *141*, 5−10.
(37) Hori, H.; Yamamoto, A.; Koike, K.; Kutsuna, S.; Murayama, M.; Yoshimoto, A.; Arakawa, R. Photocatalytic decomposition of a perfluoroether carboxylic acid by tungstic heteropolyacids in water. *Appl. Catal., B* **2008**, *82*, 58−66.
(38) Bao, Y.; Deng, S.; Jiang, X.; Qu, Y.; He, Y.; Liu, L.; Chai, Q.; Mumtaz, M.; Huang, J.; Cagnetta, G. Degradation of PFOA substitute: GenX (HFPO−DA ammonium salt): Oxidation with UV/persulfate or reduction with UV/sulfite? *Environ. Sci. Technol.* **2018**, *52*, 11728−11734.
(39) Bao, Y.; Cagnetta, G.; Huang, J.; Yu, G. Degradation of hexafluoropropylene oxide oligomer acids as PFOA alternatives in simulated nanofiltration concentrate: Effect of molecular structure. *Chem. Eng. J.* **2020**, *382*, 122866.
(40) Bentel, M. J.; Yu, Y.; Xu, L.; Li, Z.; Wong, B. M.; Men, Y.; Liu, J. Defluorination of per-and polyfluoroalkyl substances (PFASs) with hydrated electrons: Structural dependence and implications to PFAS remediation and management. *Environ. Sci. Technol.* **2019**, *53*, 3718−3728.
(41) Liu, J.; Van Hoomissen, D. J.; Liu, T.; Maizel, A.; Huo, X.; Fernández, S. R.; Ren, C.; Xiao, X.; Fang, Y.; Schaefer, C. E.; Higgins, C. P.; Vyas, S.; Strathmann, T. J. Reductive defluorination of branched per-and polyfluoroalkyl substances with cobalt complex catalysts. *Environ. Sci. Technol. Lett.* **2018**, *5*, 289−294.
(42) Seppelt, K. Trifluoromethanol, CF_3OH. *Angew. Chem., Int. Ed.* **1977**, *16*, 322−323.
(43) Christe, K. O.; Hegge, J.; Hoge, B.; Haiges, R. Convenient access to trifluoromethanol. *Angew. Chem., Int. Ed.* **2007**, *46*, 6155−6158.
(44) Suenram, R. D.; Lovas, F. J.; Pickett, H. M. Fluoromethanol: Synthesis, microwave spectrum, and dipole moment. *J. Mol. Spectrosc.* **1986**, *119*, 446−455.
(45) Maza, W. A.; Breslin, V. M.; Plymale, N. T.; DeSario, P. A.; Epshteyn, A.; Owrutsky, J. C.; Pate, B. B. Nanosecond transient absorption studies of the pH-dependent hydrated electron quenching by HSO_3^-. *Photochem. Photobiol. Sci.* **2019**, *18*, 1526−1532.
(46) Sun, Z.; Zhang, C.; Xing, L.; Zhou, Q.; Dong, W.; Hoffmann, M. R. UV/nitrilotriacetic acid process as a novel strategy for efficient photoreductive degradation of perfluorooctanesulfonate. *Environ. Sci. Technol.* **2018**, *52*, 2953−2962.
(47) Park, H.; Vecitis, C. D.; Cheng, J.; Dalleska, N. F.; Mader, B. T.; Hoffmann, M. R. Reductive degradation of perfluoroalkyl compounds with aquated electrons generated from iodide photolysis at 254 nm. *Photochem. Photobiol. Sci.* **2011**, *10*, 1945−1953.
(48) Tian, H.; Gao, J.; Li, H.; Boyd, S. A.; Gu, C. Complete defluorination of perfluorinated compounds by hydrated electrons generated from 3-indole-acetic-acid in organomodified montmorillonite. *Sci. Rep.* **2016**, *6*, 32949.
(49) Song, Z.; Tang, H.; Wang, N.; Zhu, L. Reductive defluorination of perfluorooctanoic acid by hydrated electrons in a sulfite-mediated UV photochemical system. *J. Hazard. Mater.* **2013**, *262*, 332−338.

https://dx.doi.org/10.1021/acs.est.9b05869
Environ. Sci. Technol. 2020, 54, 2489−2499